J Solid State Electrochem (2012) 16:2217–2226
DOI 10.1007/s10008-012-1647-1

ORIGINAL PAPER

Oxidation of dopamine on multi-walled carbon nanotubes

Nikos G. Tsierkezos · Uwe Ritter

Received: 24 August 2011 / Revised: 24 October 2011 / Accepted: 4 January 2012 / Published online: 26 January 2012

Abstract Novel films consisting of multi-walled carbon nanotubes (MWCNTs) were fabricated by means of the chemical vapor deposition technique with decomposition of either acetonitrile (ACN) or benzene (BZ) in the presence of ferrocene ($FeCp_2$) which served as catalyst. The electrochemical response of the two different kinds of MWCNT-based films, further referred to as MWCNT-ACN and MWCNT-BZ, towards the oxidation of dopamine (DA) to dopamine-o-quinone (DAQ) was tested by means of cyclic voltammetry, differential pulse voltammetry, and electrochemical impedance spectroscopy. Both MWCNT-based films exhibit quasi-reversible response towards DA/DAQ with some slight kinetic differences; specifically, the charge-transfer process was found to be faster on MWCNT-ACN ($k_s=35.3\times10^{-3}$ cm s^{-1}) compared to MWCNT-BZ ($k_s=6.55\times10^{-3}$ cm s^{-1}). The detection limit of MWCNT-BZ for DA (0.30 μM) appears to be poorer compared to that of MWCNT-ACN (0.03 μM), but nevertheless, both MWCNT-based films exhibit greater detection ability compared to other electrodes reported in the literature. The sensitivities of MWCNT-ACN and MWCNT-BZ towards DA/DAQ were determined as 0.65 and 0.22 A M^{-1} cm^{-2}, respectively. The findings suggest that the fabricated MWCNT-based electrodes can be successfully applied for the detection of molecules with biological interest.

Keywords Chemical vapor deposition · Differential pulse voltammetry · Dopamine · Electrochemical impedance spectrometry · Multi-walled carbon nanotubes

N. G. Tsierkezos (✉) · U. Ritter
Department of Chemistry, Ilmenau University of Technology,
Weimarer Straße 25,
98693 Ilmenau, Germany
e-mail: nikos.tsierkezos@tu-ilmenau.de

Introduction

Biosensors constructed at the molecular scale represent the most exciting application area in nanobiotechnology since they are extremely sensitive, selective, and reactive [1]. The nanotechnology-based biosensors are particularly suitable in the medical diagnostics area since they can be used in order to replace the more costly and tedious laboratory methods for checking the patient's blood for proteins, chemicals, and pathogens. For the development of electrochemical biosensors, multi-walled carbon nanotubes (MWCNTs) are usually used because of their numerous benefits, namely their high electrochemically accessible surface area, rich functionalization chemistry, high electrical conductivity, as well as the very useful mechanical properties. Furthermore, MWCNTs can be successfully used as non-enzymatic sensors for selective detection of biomolecules with high sensitivity and stability [2].

Dopamine or 2-(3,4-dihydroxyphenyl)ethylamin, with the chemical formula of $(OH)_2C_6H_3–CH_2–CH_2–NH_2$ (further abbreviated as DA) is a member of the catecholamine family and one of the best known neurotransmitter, which activates five known types of dopamine receptors (D_1–D_5) and their variants [3]. DA was first synthesized by Barger and Ewens [4], but its function as a neurotransmitter was initially recognized by Carlsson [5–7], who was awarded the Nobel Prize in Physiology or Medicine in 2000 for showing that DA is not just a precursor of norepinephrine and epinephrine but also a neurotransmitter. DA is biosynthesized through the decarboxylation of 3,4-dihydroxyphenylalanine (L-DOPA) by the enzyme aromatic-L-amino-acid decarboxylase (L-AADC) [8]. In details, the process of the synthesis of DA occurs in two main steps: initially L-DOPA is formed via hydroxylation of the amino acid L-tyrosine in the presence of the enzyme tyrosine hydroxylase, which is finally converted to DA via decarboxylation in the presence of the

enzyme L-AADC. In some neurons, DA is further converted in the presence of dopamine beta-hydroxylase to norepinephrine, which is transformed to epinephrine by the enzyme phenylethanolamine *N*-methyltransferase. DA has a wide variety of functions in the brain, including important roles in pleasure, behavior, cognition, controlled movement, motivation, sleep, mood, attention, working memory, and learning. In other words DA regulates the flow of information and affects the way that the brain controls our movement. It is strongly associated with the pleasure system in the brain, and its release provides feelings of enjoyment and supports the activities that provide those feelings. Disorders in DA levels cause declines in neurocognitive functions like memory, attention, and problem solving. Furthermore, lack of DA results in Parkinson's disease and other related disorders. To increase the amount of DA in the brains of patients with such diseases, the precursor of DA, namely L-DOPA, is usually given, since DA cannot cross the blood–brain barrier, and thus, it does not directly affect the central nervous system [9]. An understanding of the electrochemical processes of DA would be very useful for the development of analytical methods for the diagnosis of some diseases. It is well known that in clinical medicine, it is often advantageous to develop an electro-analytical method for studying electron transfer processes. Numerous studies of the electrochemical behavior of DA and its analogs, such as epinephrine, were already reported in the literature [10–14]. As was already suggested, the oxidation of DA can be characterized as a two-electron transfer process which leads to the formation of the corresponding di-ketone, namely dopamine-o-quinone (further referred to as DAQ), according to the following reaction:

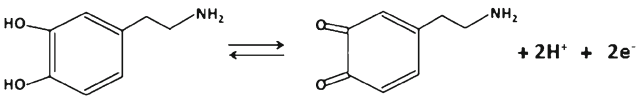

(1)

Our research activities were currently involved in the development of MWCNT-based electrodes by means of the chemical vapor deposition (CVD) technique. We have actually developed novel and rapid-response sensors based on carbon nanotube arrays, which are able to detect selectively, down to micromole concentrations, either organometallic compounds or organic molecules [15–18]. In the present work, we extend our research activity into electrochemical studies on biomolecules on MWCNT-based sensors. Specifically, the aim of the research work is the investigation of the electrochemical response of the novel fabricated MWCNT-based sensors towards the electrooxidation of DA. The obtained results reveal that the novel MWCNT-based electrodes exhibit rapid response and high sensitivity towards the DA/DAQ redox couple and, consequently, open the possibility of using MWCNT as materials in biomolecule sensing.

Experimental

Reagents

All chemicals were of analytical grade and were used as received without further purification. Dopamine, $(HO)_2C_6H_3$–CH_2–CH_2–NH_2·HCl (>99.0%) was purchased from Aldrich, while ferrocene, $(C_5H_5)_2Fe$ (>98.0%) was purchased from Fluka. The aqueous buffer solutions were prepared immediately prior to the electrochemical experiments by using double-distilled water having a specific conductivity of 0.1 μS cm^{-1}. All measurements were carried out at pH=7.0 by using phosphate buffer solution. Solutions of DA of the desired concentration were prepared daily. The phosphate buffer solution containing NaCl (8.0 gL^{-1}), KCl (0.2 gL^{-1}), Na_2HPO_4 (3.26 gL^{-1}), and KH_2PO_4 (Xg L^{-1}) was set to the wished pH by varying the X mass of KH_2PO_4.

Apparatus and procedures

Cyclic voltammograms (CVs) and differential pulse voltammograms (DPVs) were recorded using a computer-controlled system, Zahner/IM6/6EX, and analyzed by means of Thales software (version 4.15). The measurements were carried out using a three-electrode cell configuration. The working electrode used was either MWCNT-acetonitrile (ACN) (active surface area, 3.09 cm^2) or MWCNT-benzene (BZ) (active surface area, 1.57 cm^2) film, and the counter electrode was Pt plate (geometric area, 2.0 cm^2). All potentials were recorded relative to Ag/AgCl (KCl sat.) reference electrode, and thus, all potential values reported in this article are referred to this reference electrode. A three-compartment electrochemical cell designed to minimize the distances between the electrodes with a total volume of 20 mL was used for all measurements. Before each measurement, the measured solution was purged with high-purity argon to eliminate interference from dissolved oxygen. The CVs were recorded in the potential range from −0.4 to 1.0 V (vs. Ag/AgCl) with scan rates (v) ranging from 0.05 to 0.10 Vs^{-1}. DPV curves were recorded in potential range from 0 to 0.5 V (vs. Ag/AgCl) at the potential scan rate v=0.02 Vs^{-1}. The other DPV parameters were the following: pulse amplitude, 10 mV; step height, 5 mV; pulse width, 50 ms; pulse height, 50 mV; time of integration, 50 ms; and settling time, 2 s. All measurements were carried out at room temperature (21 °C).

Electrochemical impedance spectra (EIS) were recorded using the computer-controlled system Zahner/IM6/6EX by applying small ac amplitude (10 mV) in the frequency range

from 0.1 Hz to 100 kHz at 21 °C. All measurements were performed on either MWCNT-ACN (3.09 cm^2) or MWCNT-BZ (1.57 cm^2) working electrodes against the reference electrode Ag/AgCl (KCl sat.), while a Pt plate (2.0 cm^2) was served as counter electrode. In all cases, the EIS were recorded at a potential corresponding to the half-wave potential ($E_{1/2}$) of the investigated electro-active compound. The EIS data were analyzed using the Thales software (version 4.15).

Scanning electron microscopy (SEM) images of MWCNT-based films were obtained on FEI/Philips (model XL30 ESEM) computer-controlled scanning electron microscope with an accelerating voltage of 10 kV and magnification factors in the range of ×1,000–×6,000.

Preparation and characterization of MWCNT-based films

Vertically aligned MWCNT were selectively grown on oxidized porous silicon wafer with a geometrical area of 1.0 cm^2 in a furnace at 900 °C by means of the catalytic CVD technique using ferrocene ($FeCp_2$) as catalyst and either ACN or BZ as carbon source [19]. In detail, a solution of $FeCp_2$ (1% *w*/*w*) in either ACN or BZ was prepared and introduced to the furnace at the temperature of 900 °C through a syringe with a flow rate of 0.2 mL min^{-1}. From the decomposition of either ACN or BZ in the presence of iron particles formed during pyrolysis, the MWCNT are formed. In order to construct the MWCNT-working electrode for the electrochemical measurements, the MWCNT-based film produced was connected to a platinum wire by using silver conducting coating. Once the silver coating was dried (after 24 h), the silver conducting part of the electrode was fully covered with varnish protective coating. The MWCNT-based film was electrochemically cleaned prior to each use by using a 0.10-mol L^{-1} solution of HCl. The scheme of the CVD apparatus and experimental details concerning this technique were already reported in previous published articles [20, 21]. The active surface of the MWCNT-ACN (3.09 cm^2) and MWCNT-BZ films (1.57 cm^2) was determined by means of CV using the standard redox couple $[Fe(CN)_6]^{3-/4-}$. For the determination of the electrode active surface, the slope of the linear variation of the anodic peak current with the square root of the scan rate (Randles–Sevcik equation) was used [22]. For the estimation, the diffusion coefficient value of $D=8.96\cdot10^{-6}$ cm^2 s^{-1} was used for $[Fe(CN)_6]^{3-/4-}$ [23]. It must be mentioned that on MWCNT-based films, well-defined CV curves of $[Fe(CN)_6]^{3-/4-}$ were obtained with peak-to-peak potential separation equal to that which corresponds to Nernstian one-electron transfer reaction ($\Delta E_p \approx 0.059$ V) [24]. Furthermore, the detection limit of MWCNT-based films on $[Fe(CN)_6]^{3-/4-}$ was determined to be about 0.80 μM, which was much better compared to that determined on other electrodes reported in literature [25]. SEM was used for the analysis of the structure and surface of MWCNT-based films. The SEM images reveal that the carbon nanotubes are of high purity and uniform in diameter. Furthermore, the SEM micrographs exhibit that the synthesized MWCNT-ACN and MWCNT-BZ films are quite homogeneous and possess a thickness of about 38 and 22 μm, respectively. It is very interesting that the SEM analysis of the used electrodes after the end of the experiments reveals some defects in the surface morphology of the MWCNT-based films. Furthermore, the SEM images exhibit that a deposition of DA occurs at the surface of the films (Fig. 1).

Results and discussion

MWCNT-ACN-based film

The electrochemical response of MWCNT-ACN towards the DA/DAQ redox couple was investigated in phosphate buffer solution (pH=7.0) in the concentration range of 0.035–0.435 mM. Representative CVs recorded at the scan rate of $v=0.05$ Vs^{-1} showing the effect of the change of concentration are shown in Fig. 2a. The extracted CV parameters are reported in Table 1. The CVs illustrate that the DA/DAQ redox couple tends to be reversible with slight kinetic changes upon variation of the concentration, which can be mostly attributed to the uncompensated resistance effect. Namely, during the positive sweep, DA is oxidized to DAQ at the potential of $E_p^{ox} \approx +0.185$ V and in the negative sweep is reduced back to DA at the potential of $E_p^{red} \approx +0.121$ V. The half-wave potential ($E_{1/2}$) for the DA/DAQ redox couple calculated as $E_{1/2}=+0.153$ V (vs. Ag/AgCl) is slightly more anodic compared to that obtained on modified carbon paste microelectrode ($E_{1/2}=+0.122$ V vs. Ag/AgCl) [26]. It is, however, interesting that both oxidation and reduction peaks tend to shift to slightly more anodic and cathodic potentials, respectively, with the increase of either the concentration or the scan rate. Consequently, the anodic and cathodic peak potential separation, $\Delta E_p = E_p^{ox} - E_p^{red}$ progressively increases with the rise of either the concentration of the electro-active compound or the scan rate. Since the slow electron transfer kinetic is concentration independent while the effect of the uncompensated resistance depends on concentration, the findings indicate that the enhanced ΔE_p values obtained at high concentrations can be attributed to the resistance which remains uncompensated [27]. Anyhow, even at low concentrations and scan rates, where the uncompensated resistance effect is negligible, the ΔE_p seems to be greater than the expected theoretical ΔE_p value of $2.3RT/nF$ for $n=2$ (or $0.059/n$ V at 25 °C) [28] indicating that the electro-oxidation of DA to DAQ is quasi-reversible. The value of $\Delta E_p=0.064$ V determined for $c=0.035$ mM at $v=0.05$ Vs^{-1} leads to the electron transfer rate constant (k_s) value of $k_s=35.3\times$

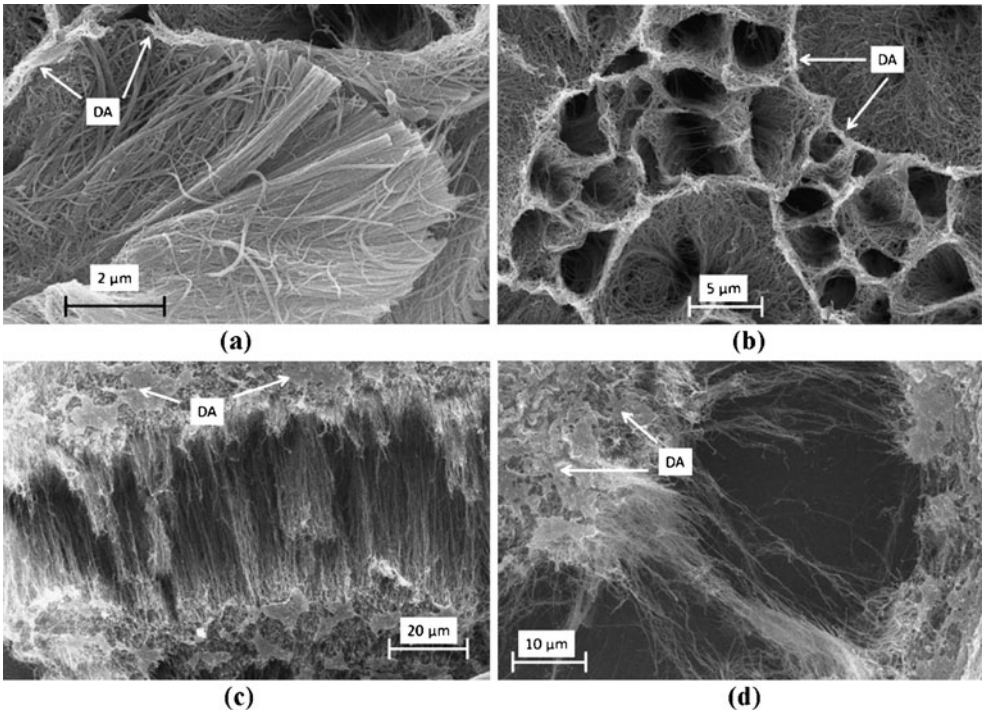

Fig. 1 SEM images of the used MWCNT-ACN **(a**, **b)** and MWCNT-BZ **(c**, **d)** films. The SEM micrographs were achieved with an accelerating voltage of 20 kV and magnification factors of ×6,000 (**a**), ×4,000 (**b**), ×1,000 (**c**), and ×2,000 (**d**)

10^{-3} cm s^{-1}. It is interesting that the k_s value of 2.21×10^{-3} cm s^{-1} obtained for DA/DAQ on modified carbon nanotube paste electrode [29] appears to be about 15 times smaller than that obtained on our novel film. Furthermore, the rate constant of $k_s=0.54\times10^{-3}$ cm s^{-1} for DA/DAQ reported for glassy carbon electrode modified with MWCNT and cobalt phthalocyanine [30] seems to be even smaller compared to the electron transfer rate constant obtained on our novel electrode ($k_s=35.3\times10^{-3}$ cm s^{-1}). The findings demonstrate that on MWCNT-based electrode, the oxidation of DA tends to be faster.

The electrochemical response of MWCNT-ACN electrode presented graphically as the variation of either the oxidation or reduction peak current with the concentration of DA was linear in the investigated concentration range of 0.035–0.435 mM (Fig. 3a) (the correlation coefficient value was 0.9998). The last finding is very interesting since the current–concentration curve may be used for the analytical determination of DA in unknown samples. We have to mention, however, that as the concentration of DA increases further, the increase in the oxidation current slows down. This phenomenon can be explained by the saturation of DA in the film, something which can be observed also in the SEM images. Namely, as it can be clearly seen in the SEM micrographs shown in Fig. 1, a deposition of DA takes place on the surface of the electrodes. Thus, the results obtained in the present work reveal that the MWCNT-ACN film has a relatively high sensitivity to DA if its concentration is below the saturation concentration in the film. It is very interesting that proportional variation of the oxidation current with the concentration of DA was also observed in the concentration range of 0.1–0.4 mM by other researchers [31]. Consequently, the linear concentration–current calibration curve obtained in the present work allowed the determination of the electrode's detection limit and sensitivity towards DA/DAQ. The limit of detection of MWCNT-ACN for DA/DAQ was determined as

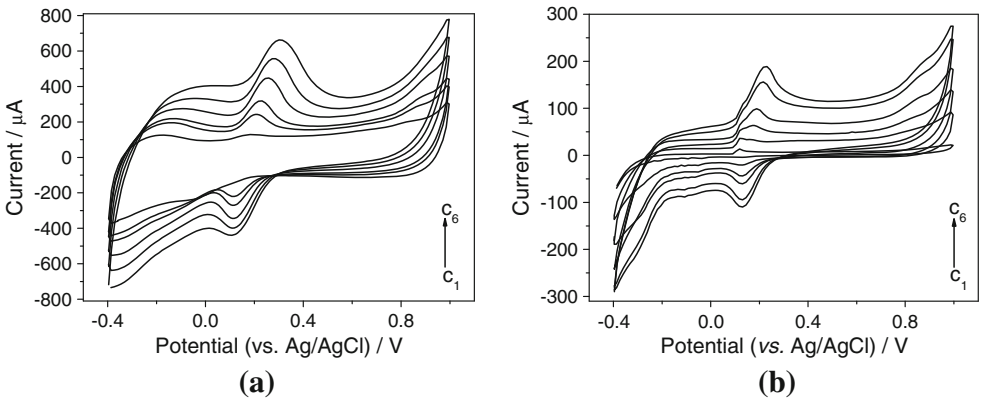

Fig. 2 CVs recorded at several DA concentrations (c_1=0.035 mM, c_2=0.099 mM, c_3=0.155 mM, c_4=0.272 mM, c_5=0.363 mM, c_6=0.435 mM) on MWCNT-ACN (**a**) and MWCNT-BZ (**b**) films at the scan rate of v=0.05 Vs^{-1}

Table 1 CV and EIS parameters obtained for the DA/DAQ redox couple on novel MWCNT-based films in phosphate buffer solutions (pH=7.0)

Electrochemical parameter	MWCNT-ACN	MWCNT-BZ
E_p^{ox}/V [a]	+0.185	+0.214
E_p^{red}/V [a]	+0.121	+0.129
$E_{1/2}$/V [a, b]	+0.153	+0.172
ΔE_p/V	0.064	0.085
i_p^{ox}/i_p^{red} [c]	1.02	1.05
$D/10^{-6}$ cm^2 s^{-1}	3.385	3.320
$k_s/10^{-3}$ cm^2 s^{-1}	35.3 [e]/34.2 [f]	6.55 [e]/7.31 [f]
$C_{dl}/10^{-3}$ F [d]	3.59	1.36
R_{ct}/Ω [d]	18	40
$C_{ad}/10^{-12}$ F [d]	16	38
R_{ad}/Ω [d]	22	51
σ/Ω s$^{-1/2}$ [d, g]	111	141
Detection limit/10^{-6} M	0.03	0.30
Sensitivity/AM^{-1} cm^{-2}	0.65	0.22

[a] All potentials are reported versus Ag/AgCl (KCl sat.) reference electrode

[b] The $E_{1/2}$ values were determined as the average values of E_p^{ox} and E_p^{red} [46]

[c] Anodic (i_p^{ox}) and cathodic (i_p^{red}) peak currents ratios

[d] The EIS parameters were determined by means of the equivalent electrical circuit ($R_s+(C_f/R_f)+(C_{dl}/(R_{ct}+(C_{ad}/R_{ad})))+Z_w$) (Fig. 5) (Thales software, version 4.15)

[e] The k_s values were determined from recorded CVs

[f] The k_s values were determined from recorded EIS spectra

[g] The Warburg parameter σ is connected with the Warburg impedance Z_W according to the relation: $Z_w=\sigma/(i\omega)^{1/2}$, where ω is the angular frequency [47]

0.03 μM at v=0.05 Vs^{-1}. Furthermore, considering that the active surface area of MWCNT-ACN is 3.09 cm^2, from the slope of the concentration–current calibration curve shown in Fig. 3a, the electrode's sensitivity of 0.65 AM^{-1} cm^{-2} was determined. To our knowledge, only three previously published studies report such small electrode's detection limits for DA. Namely, Wang et al. [32] reported that the detection limit for DA of an electrode consists of glassy carbon and $LaFeO_3$ nanoparticles is 0.03 μM, which is similar with that obtained on our novel MWCNT-ACN film. In addition, Ardakani et al. [33] reported for carbon paste electrode modified with *N*,*N*′(2,3-dihydroxybenzylidene)-1,4-phenylenediamine and TiO_2 nanoparticles a detection limit of 0.0314 μM. Furthermore, a slightly smaller detection limit (0.01 μM), compared to that obtained on MWCNT-ACN (0.03 μM), was reported by Xu et al. [34] for glassy carbon electrode modified with electropolymerized bromothymol blue. However, it would be very interesting to compare the detection ability of our novel MWCNT-based electrode with that of other electrodes reported in the literature. It was observed that the novel MWCNT-ACN film fabricated in the present work exhibits generally significantly greater detection ability towards the redox couple DA/DAQ compared to other novel electrodes reported in the literature. Specifically, Kurniawan et al. [35] reported that the detection limit for DA of an electrode consisting of gold nanoparticles is about 4.0 μM, which is greatly poorer compared to the detection limit obtained for MWCNT-ACN electrode. Furthermore, Chandrashekar et al. [36] determined a detection limit of about 10 μM for DA on carbon paste electrode modified with poly-ethylene glycol, which is significantly poorer compared to the detection limit observed on our MWCNT-ACN film. In addition, Min and Yoo [37] reported that the detection ability of single-walled carbon nanotube (SWCNT) film modified with poly-pyrrole towards the DA/DAQ redox system was 5 μM, which is also considerably poorer compared to that determined on our novel MWCNT-ACN electrode. Also interesting is that these authors reported for the modified SWCNT-based film a sensitivity of 0.467 AM^{-1} cm^{-2} which is rather smaller compared to the sensitivity obtained for MWCNT-ACN (0.65 A M^{-1} cm^{-2}). It is also remarkable that MWCNT electrode modified with poly-aniline exhibits the detection limit of 38 μM towards DA/DAQ which is also significantly poorer compared to that of our novel MWCNT-based films [38]. A detailed comparison of the detection limits and sensitivities of the novel MWCNT-based electrodes fabricated in the present work with a large number of other modified or unmodified electrodes reported in literature is shown in Table 2. From this

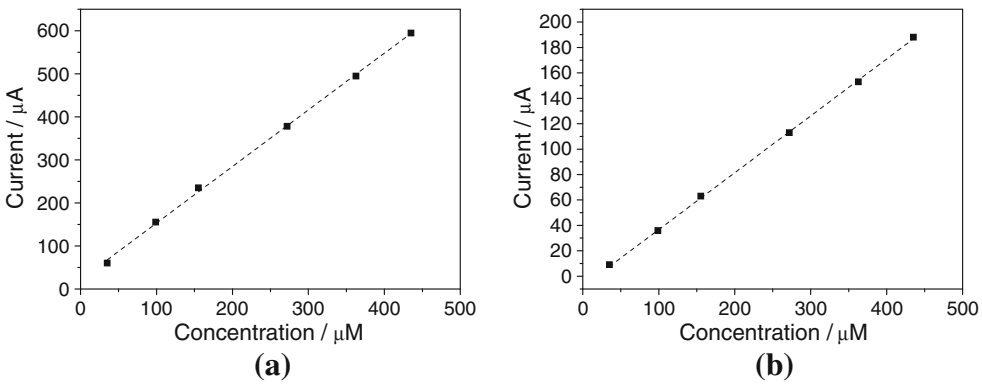

Fig. 3 Variation of the oxidation current with the DA concentration (in the range of 0.035–0.435 mM) observed in CVs recorded on MWCNT-ACN (**a**) and MWCNT-BZ (**b**) films at the scan rate of v=0.05 Vs^{-1}

Table 2 Detection limits and sensitivities of the novel MWCNT-based films and other electrodes reported in the literature towards DA/DAQ redox couple, determined by means of either CV, amperometry (AMP), DPV, or linear sweep voltammetry (LSV)

Electrode material	Method	Detection limit (10^{-6} M)	Sensitivity(A M^{-1} cm^{-2})	Reference
MWCNT-ACN[a]	CV	0.03	0.65	This work
MWCNT-BZ[a]	CV	0.30	0.22	This work
Au[b]	CV	4.0	10	Kurniawan et al. [35]
CP[c]	CV	10		Chandrashekar et al. [36]
SWCNT[d]	AMP	5.0	0.467	Min and Yoo [37]
CF[e]	CV	0.20		Hafizi et al. [48]
Au[f]	DPV	0.30		Behpour et al. [49]
GC[g]	CV	0.08		Sun et al. [50]
PT[h]	CV	0.40		Gao et al. [51]
Pt[i]	CV	20		Doyle et al. [52]
GC[j]	DPV	0.03		Ensafi et al. [53]
CP[k]	CV	0.237		Mahanthesha et al. [54]
MWCNT[l]	AMP	38		Sabzi et al. [38]
Pt[m]	CV	0.08		Jo et al. [55]
GC[n]	DPV	0.10	1.21	Huong et al. [56]
CP[o]	CV	0.45		Oni et al. [26]
CNT[p]	CV	0.087		Ardakani et al. [29]
CF[q]	DPV	0.07		Hocevar et al. [57]
GC[r]	DPV	0.20		Kamyabi et al. [58]
GC[s]	DPV	0.256		Moraes et al. [30]
Pt[t]	LSV	0.086/0.061		Atta et al. [41]
GC[u]	CV	0.03		Wang et al. [32]
CP[v]	CV	0.70		Sun et al. [59]
GC[w]	DPV	0.01		Xu et al. [34]
CF[x]	CV	0.1		Ates et al. [59]
CP[y]	DPV	0.0314		Ardakani et al. [33]

[a] Values obtained in the present work for MWCNT-based films

[b] Electrode consists of gold nanoparticles [35]

[c] Carbon paste electrode modified with poly-(ethylene glycol) [36]

[d] Single-walled carbon nanotubes modified with poly-(pyrrole) [37]

[e] Carbon fiber microelectrode [60]

[f] Gold electrode modified with 2-aminothiophenol and furfural aldehyde [48]

[g] Activated roughened glassy carbon electrode [49]

[h] Deactivated poly-thiophene film [50]

[i] Platinum electrode modified with poly-(pyrrole) [51]

[j] Glassy carbon electrode modified with poly-(sulfonazo III) [52]

[k] Carbon paste electrode modified with alizarin [53]

[l] MWCNT film modified with poly-(aniline) [38]

[m] Platinum electrode modified with single-walled carbon nanotubes and phytic acid [54]

[n] Glassy carbon electrode modified with poly-(3-methylthiophene) [55]

[o] Carbon paste microelectrode modified with iron(II)tetrasulfophthalocyanine [26]

[p] Carbon nanotube paste electrode modified with 2,2′-[1,2-ethanediylbis(nitriloethylidyne)]-bis-hydroquinone [29]

[q] Single carbon fiber microelectrode modified with MWCNT and Nafion [56]

[r] Glassy carbon electrode modified with MWCNT and bis(pyterpy)iron(II) thiocyanate complex (where pyterpy is 4′-(4-pyridyl)-2,2′:6′,2″-terpyridine) [57]

[s] Glassy carbon electrode modified with MWCNT and cobalt phthalocyanine [30]

[t] Pt electrode modified with poly-(3,4-ethylene dioxythiophene) [41]

[u] Glassy carbon electrode modified with $LaFeO_3$ nanoparticles [32]

[v] Carbon paste electrode modified with *N*-butylpyridinium hexafluorophosphate [58]

[w] Glassy carbon electrode modified with poly-(bromothymol blue) [34]

[x] Carbon fiber microelectrode modified with poly-(carbazole) [59]

[y] Carbon paste electrode modified with *N*,*N*′(2,3-dihydroxybenzylidene)-1,4-phenylenediamine and TiO_2 nanoparticles [33]

comparison, it can be clearly seem that, without any doubt, the quality of the MWCNT-based electrode produced in the present work is very good.

It is well known that the EIS technique is a useful tool for studying the interface properties of surface-modified electrodes [39, 40]. Therefore, the EIS method was used to investigate the nature of DA interaction at the surface of MWCNT-based electrode. The EIS spectra were recorded at AC frequency varying between 0.1 Hz and 100 kHZ with an applied potential in the region corresponding to the half-wave potential of the redox couple DA/DAQ. The effect of the concentration of the electro-active compound on the kinetics of the electron transfer process has been actually investigated. It is remarkable that no significant changes were observed in recorded EIS spectra with the change of DA concentration. A representative EIS spectrum recorded on MWCNT-ACN film for the most concentrated investigated DA solution (c=0.435 mM) is displayed in Fig. 4a. In the EIS spectrum shown in Fig. 4a, the complex impedance is presented as a sum of the real (Z_{re}) and the imaginary (Z_{imag}) components (as Nyquist plot). The EIS spectrum consists of a part of a semicircle in high and moderate frequency range and an anomalous straight line at a lower frequency range. For the simulation of the recorded EIS spectra, the equivalent electrical circuit (R_s+(C_f/R_f)+(C_{dl}/(R_{ct}+(C_{ad}/R_{ad})))+Z_w) was used (Fig. 5). The extracted EIS parameters are included in Table 1. The elements of the applied electrical circuit are explained as follows: R_s is the uncompensated Ohmic resistance of the cell; R_{ct}, R_f, and R_{ad} are the charge-transfer resistance, the resistance associated with the surface of the working electrode and the adsorption resistance, respectively; C_{dl}, C_f, and C_{ad} are the double-layer capacitance, the electrode surface capacitance, and the adsorption capacitance, respectively, and Z_w is the Warburg impedance. The obtained mean percent impedance and mean phase angle errors obtained from simulation were less than 0.4% and 0.1, respectively.

The charge transfer resistance (R_{ct}≈18 Ω) determined for the redox couple DA/DAQ was found to be nearly invariant within experimental error in all investigated concentrations. It is very interesting that an electrode consists of Pt modified with poly(3,4-ethylene dioxythiophene), Nyquist plots with the same shape were obtained for DA/DAQ [41]. It is as well very interesting that on this particular electrode, an extremely higher charge transfer resistance (R_{ct}≈278 Ω) was determined compared to that obtained on our novel MWCNT-based electrode (R_{ct}≈18 Ω). The findings show that our novel MWCNT-based electrode provides fewer barriers for the electron transfer process confirming thus that the quality of the electrode is very good. It is very interesting to mention that from the Warburg impedance Z_w, the corresponding Warburg coefficient (σ) for DA/DAQ on MWCNT-based electrode was determined (σ= 111 $\Omega s^{-1/2}$), a parameter which is strongly dependent on the diffusion ability of the redox species [42]. Thus, from the obtained σ value, the diffusion coefficient of D=3.385×10^{-6} cm^2 s^{-1} was determined, which is in absolute agreement within experimental error to the D values of D=3.4×10^{-6} cm^2 s^{-1} [11] and D=3.5×10^{-6} cm^2 s^{-1} [43] reported in the literature. Also interesting is that the electron transfer rate value of k_s=34.2×10^{-3} cm s^{-1} determined from the obtained charge transfer resistance value of R_{ct}≈18 Ω agrees reasonably with the k_s value of k_s=35.3×10^{-3} cm s^{-1}, obtained by means of the CV technique [44].

MWCNT-BZ-based film

Representative CVs of DA/DAQ recorded on MWCNT-BZ at the scan rate of v=0.05 V s^{-1} showing the effect of the change of concentration, are shown in Fig. 2b. The extracted CV parameters are included in Table 1. Some slight differences in the potentials and the kinetic parameters were observed for DA/DAQ on MWCNT-BZ. Specifically, the CVs recorded on this particular electrode exhibit oxidation and reduction waves at E_p^{ox}≈+0.214 V and E_p^{red}≈+0.129 V (vs. Ag/AgCl), respectively, and thus, the half-wave potential of DA/DAQ determined as $E_{1/2}$=+0.172 V (vs. Ag/AgCl) is slightly more anodic compared to $E_{1/2}$ obtained on MWCNT-ACN ($E_{1/2}$=+0.153 V vs. Ag/AgCl). Furthermore, the peak potential separation of ΔE_p=0.085 V,

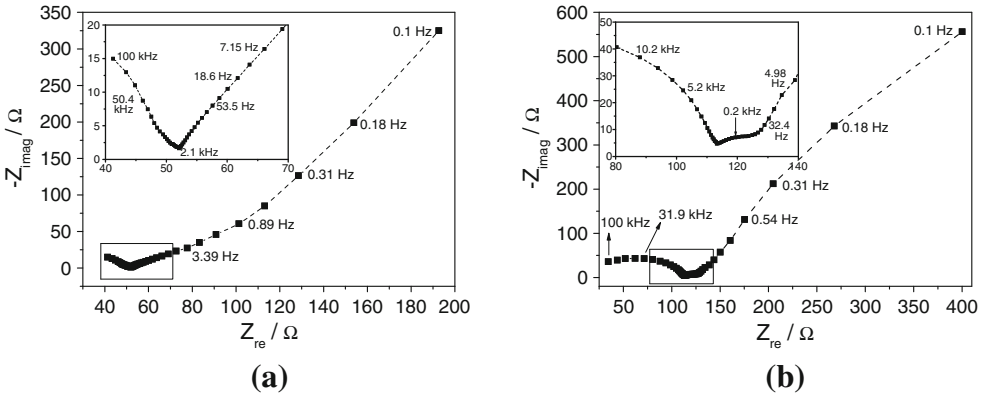

Fig. 4 EIS spectra recorded for DA (c=0.435 mM) on MWCNT-ACN (**a**) and MWCNT-BZ (**b**) films in the frequency range of 0.1 Hz–100 kHz. *Inset*: A zoom of the impedance results in high and intermediate frequency range

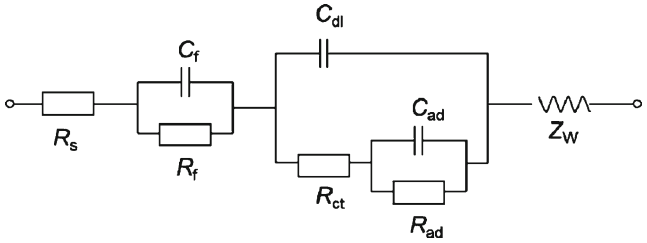

Fig. 5 Equivalent electrical circuit (R_s+(C_f/R_f)+(C_{dl}/(R_{ct}+(C_{ad}/R_{ad}))) +Z_w) used for fitting the EIS spectra for DA/MWCNT system (Thales software, version 4.15)

determined for DA/DAQ on MWCNT-BZ (c=0.035 mM, v=0.05 Vs^{-1}), seems to be greater than the value of ΔE_p= 0.064 V, obtained on MWCNT-ACN at the same concentration and scan rate. Accordingly, the charge transfer process occurring on MWCNT-BZ (k_s=6.55×10^{-3} cm s^{-1}) appears to be about five times slower compared to that taking place on MWCNT-ACN (k_s=35.3×10^{-3} cm s^{-1}). The findings can be explained through the existence of iron nanoparticles incorporated into the structure of the nanotubes, which interrupt the electro-oxidation of DA on this particular electrode. Specifically, it was observed that the recorded CVs display at low concentrations and low scan rates an additional oxidation peak at about E_p^{ox}≈+0.06 V (vs. Ag/AgCl), which can be ascribed to the iron nanoparticles. As was already reported in a previous published work, the carbon nanotubes grown with the decomposition of BZ are highly iron-doped [45]. Consequently, it can be concluded that the detection ability and the sensitivity of the MWCNT-BZ electrode weaken due to an increase of the background "noise." As it can be seen in Fig. 3b, the variation of the oxidation peak current with the concentration of the electro-active compound seems to be linear in the investigated concentration range of 0.035–0.435 mM. Consequently, from the concentration–current curve, the detection limit of 0.30 μM was estimated for MWCNT-BZ at v=0.05 Vs^{-1}. The detection limit obtained on MWCNT-BZ appears to be quite poorer compared to that determined on MWCNT-ACN (0.03 μM) at the same scan rate. Furthermore, considering that the active surface area of the MWCNT-BZ film is 1.57 cm^2, the electrode's sensitivity of 0.22 AM^{-1} cm^{-2} was calculated, which is slightly less than that determined for MWCNT-ACN (0.65 AM^{-1} cm^{-2}). In order to investigate further the detection ability of MWCNT-BZ film, DPVs were also recorded on this particular electrode in extremely low concentrations (in the range from 0.17 to 3.33 μM). The recorded DPVs are shown in Fig. 6a. It can be obviously observed in Fig. 6a that for concentrations below 0.30 μM, no oxidation current can be seen in recorded DPVs. In the investigated concentration range (0.33–3.0 μM), the variation of the oxidation current with the concentration of DA is linear (Fig. 6b) and leads to the detection limit of 0.30 μM which is in absolute agreement with that determined from the CV studies. It is very interesting to remark at this point that even if the detection ability of MWCNT-BZ is poorer than that of MWCNT-ACN, it appears to be much better compared to that of other novel electrodes reported in the literature (Table 2).

Figure 4b displays a representative Nyquist plot recorded for DA (c=0.435 mM) on MWCNT-BZ. The extracted EIS parameters are included in Table 1. The EIS spectra consist of two semicircles, namely a whole semicircle and a second semicircle with compressed shape in the high and intermediate frequency range, respectively, and an anomalous line, which appears in the lower frequency range. The greater value of charge transfer resistance (R_{ct}≈40 Ω) was determined for DA/DAQ on MWCNT-BZ indicating the bigger barrier for electron transfer process and therefore the slower kinetics which characterizes this particular electrode. This observation supports the CV results. From the determined R_{ct} value of R_{ct}≈40 Ω, the heterogeneous electron transfer rate constant of k_s=7.31×10^{-3} cm s^{-1} was estimated, which agrees reasonably within experimental error with the value of k_s=6.55×10^{-3} cm s^{-1} obtained from the recorded CVs. Furthermore, from the Warburg coefficient of σ=141 Ω$s^{-1/2}$ estimated for DA/DAQ on MWCNT-BZ, the diffusion coefficient of D=3.32×10^{-6} cm^2 s^{-1} was determined for

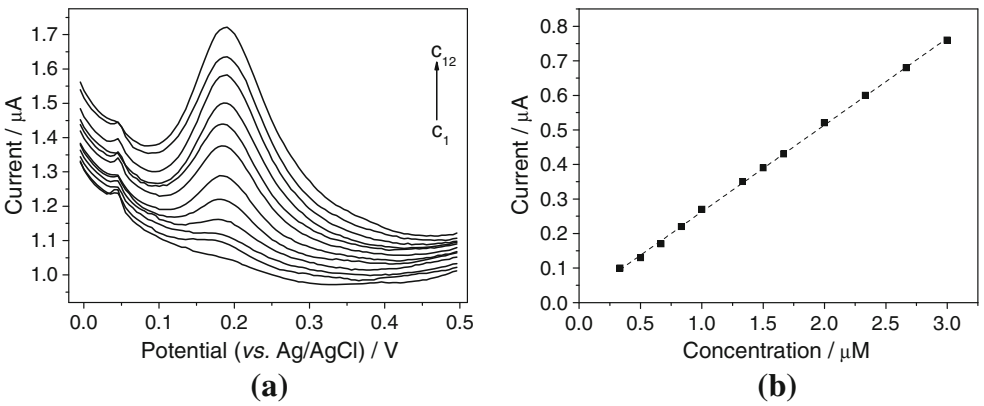

Fig. 6 **a** DPVs recorded at several DA concentrations (c_1= 0.17 μM, c_2=0.33 μM, c_3= 0.50 μM, c_4=0.67 μM, c_5= 0.83 μM, c_6=1.0 μM, c_7= 1.17 μM, c_8=1.5 μM, c_9= 1.67 μM, c_{10}=2.0 μM, c_{11}= 2.33 μM, c_{12}=3.0 μM) on MWCNT-BZ at the scan rate of v=0.02 Vs^{-1}; **b** variation of the oxidation current with the DA concentration (in the range of 0.17–3.0 μM) observed in DPVs recorded on MWCNT-BZ

DA, which agrees very well with the value of $D=3.385\times 10^{-6}$ cm^2 s^{-1} determined on MWCNT-ACN.

Conclusions

The novel MWCNT-ACN and MWCNT-BZ films were fabricated by means of the CVD technique with decomposition of ACN and BZ, respectively, and used as working electrodes for the electrochemical oxidation of DA in buffer phosphate solutions (pH=7.0). Both MWCNT-based films exhibit quasi-reversible response towards DA/DAQ with some slight kinetic differences. Namely, the charge transfer process occurring on MWCNT-BZ ($k_s=6.55\times 10^{-3}$ cm s^{-1}) is about five times slower than that taking place on MWCNT-ACN ($k_s=35.3\times 10^{-3}$ cm s^{-1}). Furthermore, the detection ability (0.30 μM) and electrode's sensitivity (0.22 AM^{-1} cm^{-2}) estimated for MWCNT-BZ towards DA/DAQ are smaller compared to those obtained for MWCNT-ACN (0.03 μM, 0.65 AM^{-1} cm^{-2}). The weaker detection ability of MWCNT-BZ can be attributed to the iron nanoparticles incorporated into the structure of the nanotubes. It is, nevertheless, very interesting that the novel MWCNT-based films fabricated in the present work exhibit higher sensitivity and lower detection limits compared to the large number of other electrodes reported in the literature. The last observation indicates the importance of using carbon nanotubes as materials for constructing bio-sensing electrodes.

Acknowledgments The authors would like to thank Mrs. D. Schneider (TU Ilmenau).

References

1. Zhang X, Guo Q, Cui D (2009) Recent advances in nanotechnology applied to biosensors. Sensors 9:1033–1053
2. Zhang WD, Chen J, Jiang LC, Yu YX, Zhang JQ (2010) A highly sensitive nonenzymatic glucose sensor based on NiO-modified multi-walled carbon nanotubes. Microchim Acta 168:259–265
3. Cornil CA, Balthazart J, Motte P, Massotte L, Seutin V (2002) Dopamine activates noradrenergic receptors in the preoptic area. J Neurosci 22:9320–9330
4. Fahn S (2008) The history of dopamine and levodopa in the treatment of Parkinson's disease. Movement Disord 23:497–508
5. Montagu KA (1957) Catechol compounds in rat tissues and in brains of different animals. Nature 180:244–245
6. Carlsson A, Waldeck B (1958) A fluorimetric method for the determination of dopamine (3-hydroxytyramine). Acta Physiol Scand 44:293–298
7. Benes FM (2001) Carlsson and the discovery of dopamine. Trends Pharmacol Sci 22:46–47
8. Sourkes TL (1966) Dopa decarboxylase: substrates, coenzyme, inhibitors. Pharmacol Rev 18:53–60
9. Neff NH, Hadjiconstantinou M (1995) Aromatic L-amino acid decarboxylase modulation and Parkinson's disease. Prog Brain Res 106:91–97
10. Xue KH, Tao FF, Xu W, Yin SY, Liu JM (2005) Selective determination of dopamine in the presence of ascorbic acid at the carbon atom wire modified electrode. J Electroanal Chem 578:323–329
11. Razmi H, Agazadeh M, Habibi B (2003) Electrocatalytic oxidation of dopamine at aluminum electrode modified with nickel pentacyanonitrosylferrate films, synthesized by electroless procedure. J Electroanal Chem 547:25–33
12. Zen JM, Chen IL (1997) Voltammetric determination of dopamine in the presence of ascorbic acid at a chemically modified electrode. Electroanalysis 9:537–540
13. Wang Z, Liu J, Liang Q, Wang Y, Luo G (2002) Carbon nanotube-modified electrodes for the simultaneous determination of dopamine and ascorbic acid. Analyst 127:653–658
14. Raj CR, Okajima T, Ohsaka T (2003) Gold nanoparticle arrays for the voltammetric sensing of dopamine. J Electroanal Chem 543:127–133
15. Tsierkezos NG, Ritter U, Philippopoulos AI, Schröder D (2010) Electrochemical studies of the bis(triphenyl phosphine)ruthenium (II) complex, *cis*-[$RuCl_2(L)(PPh_3)_2$], with L=2-(2′-pyridyl)quinoxaline. J Coordination Chem 63:3517–3530
16. Tsierkezos NG, Ritter U (2011) Determination of impedance spectroscopic behavior of triphenylphosphine on various electrodes. Anal Lett 44:1416–1430
17. Tsierkezos NG, Szroeder P, Ritter U (2011) Application of films consisting of carbon nanoparticles for electrochemical detection of redox systems in organic solvent media. Fullerenes, Nanotubes, Carbon Nanostruct 19:505–516
18. Tsierkezos NG, Szroeder P, Ritter U (2011) Multi-walled carbon nanotubes as electrode materials for electrochemical studies of organometallic compounds in organic solvent media. Monatsh Chem 142:233–242
19. Rao CNR, Sen R (1998) Large aligned-nanotube bundles from ferrocene pyrolysis. Chem Commun 1525–1526
20. Tsierkezos NG, Ritter U (2010) Synthesis and electrochemistry of multi-walled carbon nanotube films directly attached on silica substrate. J Solid State Electrochem 14:1101–1107
21. Tsierkezos NG, Ritter U (2010) Electrochemical impedance spectroscopy and cyclic voltammetry of ferrocene in acetonitrile/acetone system. J Appl Electrochem 40:409–417
22. Chokshi K, Qutubuddin S, Hussam A (1989) Electrochemical investigation of microemulsions. J Colloid Interface Sci 129:315–326
23. Lide DR (ed) (1993-1994) CRC handbook of chemistry and physics, 74th edn. CRC Press, Boca Raton
24. Nugent JM, Santhanam KSV, Rubio A, Ajayan PM (2001) Fast electron transfer kinetics on multi-walled carbon nanotube microbundle electrodes. Nano Lett 1:87–91
25. Hirano A, Kanai M, Nara T, Sugawara M (2001) A glass capillary ultramicroelectrode with an electrokinetic sampling ability. Anal Sci 17:37–43
26. Oni J, Westbroek P, Nyokong T (2003) Electrochemical behavior and detection of dopamine and ascorbic acid at an iron(II)tetrasulfophthalocyanine modified carbon paste microelectrode. Electroanalysis 15:847–854
27. Bond AM, Oldham KB, Snook GA (2000) Use of the ferrocene oxidation process to provide both reference electrode potential calibration and a simple measurement (via semiintegration) of the uncompensated resistance in cyclic voltammetric studies in high-resistance organic solvents. Anal Chem 72:3492–3496
28. Yaghoubian H, Beitollah H, Soltani-Nejad V, Mohadesi A, Afzali D, Zamani H, Roodsaz S (2011) Simultaneous voltammetric determination of epinephrine and acetaminophene at the surface

of modified carbon nanotube paste electrode. Int J Electrochem Sci 6:1307–1316
29. Ardakani MM, Beitollahi H, Ganjipour B, Naeimi H, Nejati M (2009) Electrochemical and catalytic investigations of dopamine and uric acid by modified carbon nanotube paste electrode. Bioelectrochemistry 75:1–8
30. Moraes FC, Cabral MF, Machado SAS, Mascaro LH (2008) Electrocatalytic behavior of glassy carbon electrodes modified with multiwalled carbon nanotubes and cobalt phthalocyanine for selective analysis of dopamine in presence of ascorbic acid. Electroanalysis 20:851–857
31. Shankar SS, Swamy BEK, Chandra U, Manjunatha JG, Sherigara BS (2009) Simultaneous determination of dopamine, uric acid and ascorbic acid with CTAB modified carbon paste electrode. Int J Electrochem Sci 4:592–601
32. Wang G, Sun J, Zhang W, Jiao S, Fang B (2009) Simultaneous determination of dopamine, uric acid and ascorbic acid with $LaFeO_3$ nanoparticles modified electrode. Microchim Acta 164:357–362
33. Ardakani MM, Rajabi H, Beitollahi H, Mirjalili BBF, Akbari A, Taghavinia N (2010) Voltammetric determination of dopamine at the surface of TiO_2 nanoparticles modified carbon paste electrode. Int J Electrochem Sci 5:147–157
34. Xu X, Qihuang Lin Q, Liu A, Chen W, Weng X, Wang C, Lin X (2010) Simultaneous voltammetric determination of ascorbic acid, dopamine and uric acid using polybromothymol blue film-modified glassy carbon electrode. Chem Pharm Bull 58:788–793
35. Kurniawan F, Tsakova V, Mirsky VM (2009) Analytical applications of electrodes modified by gold nanoparticles: dopamine detection. J Nanosci Nanotechnol 9:2407–2412
36. Chandrashekar BN, Swamy BEK, Pandurangachar M, Shankar SS, Gilbert O, Manjunatha JG, Sherigara BS (2010) Electrochemical oxidation of dopamine at polyethylene glycol modified carbon paste electrode: a cyclic voltammetric study. Int J Electrochem Sci 5:578–592
37. Min K, Yoo YJ (2009) Amperometric detection of dopamine based on tyrosinase-SWNTs-Ppy composite electrode. Talanta 80:1007–1011
38. Sabzi RE, Rezapour K, Samadi N (2010) Polyaniline-multi-wall-carbon nanotube nanocomposites as a dopamine sensor. J Serb Chem Soc 75:537–549
39. Roto R, Villemure G (2002) Electrochemical impedance spectroscopy of electrodes modified with thin films of Ni-Al-Cl layered double hydroxides. J Electroanal Chem 527:123–140
40. Kim JM, Patwardhan A, Bott A, Thompson DH (2003) Preparation and electrochemical behavior of gramicidin-bipolar lipid monolayer membranes supported on gold electrodes. Biochim Biophys Acta, Biomembr 1617:10–21
41. Atta NF, Galal A, Ahmed RA (2011) Poly(3,4-ethylenedioxythiophene) electrode for the selective determination of dopamine in presence of sodium dodecyl sulfate. Bioelectrochemistry 80:132–141
42. Koeleli F, Roepke T, Hamann CH (2003) Electrochemical impedance spectroscopic investigation of CO_2 reduction on polyaniline in methanol. Electrochim Acta 48:1595–1601
43. Sabzi RE, Zare S, Farhadi K, Tabrizivand G (2005) Electrocatalytic oxidation of dopamine at sol-gel carbon composite electrode chemically modified with copper hexacyanoferrate. J Chin Chem Soc 52:1079–1084
44. Sundfors F, Bobacka J, Ivaska A, Lewenstam A (2002) Kinetics of electron transfer between $Fe(CN)_6^{3-/4-}$ and poly(3,4-ethylenedioxythiophene) studied by electrochemical impedance spectroscopy. Electrochim Acta 47:2245–2251
45. Szroeder P, Tsierkezos NG, Scharff P, Ritter U (2010) Electrocatalytic properties of carbon nanotube carpets grown on Si-wafers. Carbon 48:4489–4496
46. Tsierkezos NG (2007) Cyclic voltammetric studies of ferrocene in nonaqueous solvents in the temperature range from 248.15 to 298.15 K. J Solution Chem 36:289–302
47. Tsierkezos NG, Philippopoulos AI, Ritter U (2010) Electrochemical impedance spectroscopy and cyclic voltammetry of *cis*-[Cr $(bipy)_2(SCN)_2$]I (where bipy:2,2′-bipyridine) in polar solvents. J Solution Chem 39:897–908
48. Behpour M, Ghoreishi SM, Honarmand E (2011) Aminothiophenol furfural self-assembled gold electrode sensor for determination of dopamine in pharmaceutical formulations. J Phys Chem Electrochem 1:117–122
49. Sun H, Zang C, Lian K (2009) Electrochemical behavior and determination of dopamine and ascorbic acid by cyclic voltammetry using an activated roughened glassy carbon electrode. Asian J Pharm Sci 4:200–206
50. Gao Z, Yap D, Zhang Y (1998) Voltammetric determination of dopamine in a mixture of dopamine and ascorbic acid at a deactivated polythiophene film modified electrode. Anal Sci 14:1059–1063
51. Doyle R, Breslin CB, Rooney AD (2009) A simple but highly selective electrochemical sensor for dopamine. Chem Biochem Eng Q 23:93–98
52. Ensafi AA, Taei M, Khayamian T, Arabzadeh A (2010) Highly selective determination of ascorbic acid, dopamine, and uric acid by differential pulse voltammetry using poly(sulfonazo III) modified glassy carbon electrode. Sens Actuators B 147:213–221
53. Mahanthesha KR, Swamy BEK, Pai KV, Chandra U, Sherigara BS (2010) Cyclic voltammetric investigations of dopamine at alizarin modified carbon paste electrode. Int J Electrochem Sci 5:1962–1971
54. Jo S, Jeong H, Bae SR, Jeon S (2008) Modified platinum electrode with phytic acid and single-walled carbon nanotube: Application to the selective determination of dopamine in the presence of ascorbic and uric acids. Microchem J 88:1–6
55. Huong VT, Shimanouchi T, Quan DP, Umakoshi H, Viet PH, Kuboi R (2009) Polymethylthiophene/Nafion-modified glassy carbon electrode for selective detection of dopamine in the presence of ascorbic acid. J Appl Electrochem 39:2035–2042
56. Hocevar SB, Wang J, Deo RP, Musameh M, Ogorevc B (2005) Carbon nanotube modified microelectrode for enhanced voltammetric detection of dopamine in the presence of ascorbate. Electroanalysis 17:417–422
57. Kamyabi MA, Narimani O, Monfared HH (2011) Electroless deposition of bis(4′-(4-pyridyl)-2,2′:6′,2″-terpyridine)iron(II) thiocyanate complex onto carbon nanotubes modified glassy carbon electrode: application to simultaneous determination of ascorbic acid, dopamine and uric acid. J Braz Chem Soc 22:468–477
58. Sun W, Yang M, Jiao K (2007) Electrocatalytic oxidation of dopamine at an ionic liquid modified carbon paste electrode and its analytical application. Anal Bioanal Chem 389:1283–1291
59. Ates M, Sarac AS, Turhan CM, Ayaz NE (2009) Polycarbazole modified carbon fiber microelectrode: surface characterization and dopamine sensor. Fibers Polym 10:46–52
60. Hafizi S, Kruk ZL, Stamford JA (1990) Fast cyclic voltammetry: improved sensitivity to dopamine with extended oxidation scan limits. J Neurosci Meth 33:41–49